Effects on General Acid Catalysis from Mutations of the Invariant Tryptophan and Arginine Residues in the Protein Tyrosine Phosphatase from *Yersinia*†

Richard H. Hoff,‡ Alvan C. Hengge,*,‡ Li Wu,§ Yen-Fang Keng,§ and Zhong-Yin Zhang*,§

Department of Chemistry and Biochemistry, Utah State University, Logan, Utah 84322-0300, and Department of Molecular Pharmacology, Albert Einstein College of Medicine, 1300 Morris Park Avenue, Bronx, New York 10461

Received July 7, 1999; Revised Manuscript Received October 12, 1999

ABSTRACT: General acid catalysis in protein tyrosine phosphatases (PTPases) is accomplished by a conserved Asp residue, which is brought into position for catalysis by movement of a flexible loop that occurs upon binding of substrate. With the PTPase from *Yersinia*, we have examined the effect on general acid catalysis caused by mutations to two conserved residues that are integral to this conformation change. Residue Trp354 is at a hinge of the loop, and Arg409 forms hydrogen bonding and ionic interactions with the phosphoryl group of substrates. Trp354 was mutated to Phe and to Ala, and residue Arg409 was mutated to Lys and to Ala. The four mutant enzymes were studied using steady state kinetics and heavy-atom isotope effects with the substrate *p*-nitrophenyl phosphate. The data indicate that mutation of the hinge residue Trp354 to Ala completely disables general acid catalysis. In the Phe mutant, general acid catalysis is partially effective, but the proton is only partially transferred in the transition state, in contrast to the native enzyme where proton transfer to the leaving group is virtually complete. Mutation of Arg409 to Lys has a minimal effect on the K_m, while this parameter is increased 30-fold in the Ala mutant. The k_{cat} values for R409K and for R409A are about 4 orders of magnitude lower than that for the native enzyme. General acid catalysis is rendered inoperative by the Lys mutation, but partial proton transfer during catalysis still occurs in the Ala mutant. Structural explanations for the differential effects of these mutations on movement of the flexible loop that enables general acid catalysis are presented.

The catalytic power of many enzymes is intimately connected to their ability to undergo conformational changes that can allow the repositioning of catalytic groups during catalysis. An example is the family of protein tyrosine phosphatases, which utilize a general acid to protonate the leaving group in the phosphoryl transfer reaction (*1*). The general acid, a conserved Asp residue, resides on a flexible loop that is brought into the active site by a conformational change induced by substrate binding. In this work, we have examined in detail changes in the transition state for catalysis that result from mutations to two residues that affect the conformational change controlling general acid catalysis in the *Yersinia* PTPase.[1]

PTPases have an essential role in signal transduction, and together with protein tyrosine kinases control the phosphorylation level of proteins in the cell. The *Yersinia* PTPase is one member of this enzyme family, which in common with all members of the PTPase family shares the active site signature motif C(X_5)R(S/T) (*2*). PTPases share a common catalytic mechanism (Figure 1), utilizing a Cys nucleophile (Cys403 in the *Yersinia* PTPase) in the formation of a thiophosphoryl covalent enzyme intermediate, which undergoes hydrolysis in a second step (*2*−*4*). The invariant Arg residue (Arg409 in *Yersinia* PTPase) functions in substrate binding and in transition state stabilization (*2*). The initial phosphoryl transfer step is assisted by general acid catalysis by the conserved Asp (Asp356 in the *Yersinia* PTPase) which protonates the leaving group (*5*). The Asp resides on a flexible loop that undergoes a major conformational change upon binding of substrate, or upon binding of small anions such as tungstate (*6*). This loop is termed the WpD loop for the conserved Trp-Pro-Asp sequence. The overall catalytic mechanism, including the conformational change involving WpD loop movement, is shown in Scheme 1.

Crystallographic structural data show that Trp354 is located at one of the hinge positions of the WpD loop and has interactions with Arg409 that are important in closure of the loop upon binding of substrate or structurally analogous small anions (*7*). Kinetic studies have confirmed that mutations to Trp354 result in impaired catalytic efficiency (*8*). The W354F and W354A mutants exhibit k_{cat} values that are decreased 200- and 480-fold, respectively, from that of the native enzyme using *p*-nitrophenyl phosphate (*p*NPP) as the substrate, while the K_m is relatively unaffected by these mutations. The pH dependence of these mutants

† Financial support of this work came from NIH Grants GM47297 to A.C.H. and CA69202 to Z.-Y.Z. and from the U.S. Army Advanced Civil Schooling Program for support of R.H.H. Z.-Y.Z. is a Sinsheimer Scholar and an Irma T. Hirschl Career Scientist.

* To whom correspondence should be addressed.

‡ Utah State University.

§ Albert Einstein College of Medicine.

[1] Abbreviations: *p*NPP, *p*-nitrophenyl phosphate; PTPase, protein tyrosine phosphatase; EDTA, ethylenediaminetetraacetic acid; TRIS, tris(hydroxymethyl)aminomethane; CHES, 2-(*N*-cyclohexylamino)-ethanesulfonic acid; IPTG, isopropyl β-D-thiogalactopyranoside. The notation used to express isotope effects is that of Northrop where a leading superscript of the heavier isotope is used to indicate the isotope effect on the following kinetic quantity; for example, $^{15}k_3$ denotes $^{14}k_3/^{15}k_3$, the ^{15}N isotope effect on the rate constant k_3.

10.1021/bi991570i CCC: $19.00
Published on Web 12/09/1999

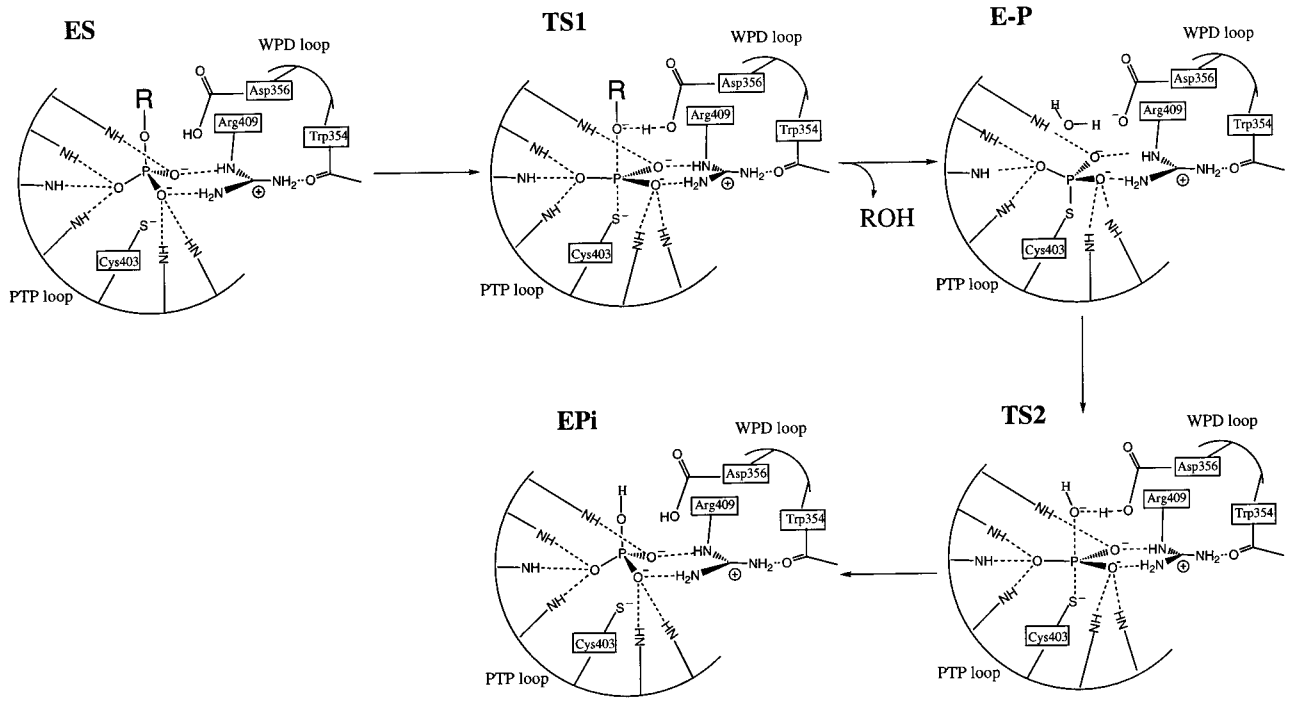

FIGURE 1: Chemical mechanism for the *Yersinia* PTPase-catalyzed hydrolysis of aryl phosphates. ES, enzyme−substrate complex; TS1, transition state for the phosphoenzyme formation step; ROH, phenol; E−P, phosphoenzyme intermediate; TS2, transition state for the hydrolysis of the phosphoenzyme intermediate; EPi, enzyme−inorganic phosphate complex.

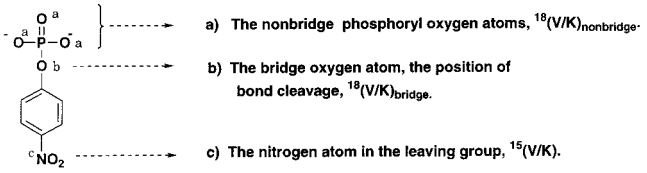

FIGURE 2: *p*-Nitrophenyl phosphate substrate used for isotope effect studies, with the positions labeled at which isotope effects were measured.

suggests that these mutations affect the competence of general acid catalysis, most likely by interfering with movement of the WpD loop on which the general acid resides (*8*).

In this study, we report kinetic studies to examine the result of mutations of Arg409, and heavy-atom isotope effects to study the mechanistic consequences of mutations to Trp354 and Arg409. The substrate for the isotope effect measurements was *p*NPP, which is shown in Figure 2 with the positions marked at which isotope effects have been measured. Prior studies of the reactions of PTPases with this substrate show that isotope effects in all three positions are sensitive to the presence or lack of general acid catalysis in the transition state (*9*−*11*). The isotope effects reveal details of how the mutations in the hinge residue Trp354 and the substrate recognition residue Arg409 affect general acid catalysis, which requires proper movement of the flexible loop. If loop movement is impaired, either the general acid could be rendered inoperative or it may be able to assume a position in which only partial proton transfer is accomplished in the transition state. Comparisons of these isotope effect results with previously reported data from the reaction of the native enzyme and of general acid mutants reveal details of the mechanistic consequences of these mutations.

MATERIALS AND METHODS

Synthesis of Compounds. [^{14}N]-*p*-Nitrophenyl phosphate, [^{15}N,nonbridge-$^{18}O_3$]-*p*-nitrophenyl phosphate, [^{14}N]-*p*-nitrophenol, and [^{15}N,^{18}O]-*p*-nitrophenol were synthesized as described previously (*12*). [^{14}N]-*p*-Nitrophenol and [^{15}N,^{18}O]-*p*-nitrophenol were then mixed to reconstitute the natural abundance of ^{15}N, and then the mixture was phosphorylated to produce *p*-nitrophenyl phosphate using the same method described above. This mixture was used for determination of $^{18}(V/K)_{bridge}$. The [^{14}N]-*p*-nitrophenyl phosphate and [^{15}N,-nonbridge-$^{18}O_3$]-*p*-nitrophenyl phosphate were also mixed to reconstitute the natural abundance of ^{15}N. This mixture was used for determination of $^{18}(V/K)_{nonbridge}$. The isotopic abundance of the mixtures was determined by isotope ratio mass spectrometry. The $^{15}(V/K)$ isotope effects were measured using natural abundance *p*NPP prepared from commercial *p*-nitrophenol and $POCl_3$ (*13*).

Enzyme Preparation. The wild type *Yersinia* PTPase and *Yersinia* PTPase mutants W354A, W354F, R409A, and R409K were expressed under the control of the T7 promoter in *Escherichia coli* BL21(DE3) cells and grown at room temperature after induction with 0.4 mM IPTG. All recombinant proteins were purified to >95% purity as described previously (*2*, *8*). The enzyme concentration was determined from the absorbance at 280 nm using an $A_{1mg/mL}^{280}$ (absor-

Scheme 1

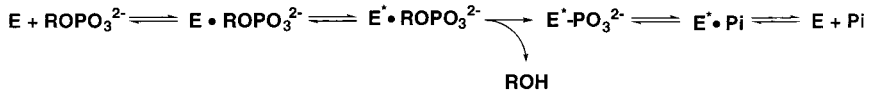

bance at 280 nm for a 1 mg/mL solution) of 0.493 for the wild type *Yersinia* PTPase and the R409A and R409K mutants. The W354A and the W354F mutant *Yersinia* PTPases have $A_{1mg/mL}^{280}$ values of 0.24 because of the substitution of the tryptophan residue.

Isotope Effect Determinations. Isotope effect experiments were carried out with 100 mM buffer and 1 mM EDTA. The buffer solutions and corresponding pH ranges were as follows: pH 5−6, acetate; pH 6−7, succinate; pH 8−9.5, TRIS; and pH 10, CHES. Typical isotope effects experiments were performed with a 10 mL reaction volume at a substrate concentration of about 15 mM. Small-scale experiments were carried out to determine the quantity of enzyme required to hydrolyze one-third to one-half of the substrate in a reasonable amount of time (generally less than 24 h) before the activity of the enzyme declined significantly. Reactions were begun with ≥100 μmol of the substrate, and sufficient enzyme was used so that background hydrolysis rates were less than 10% of the enzymatic rate. Parallel experiments without enzyme were used to establish background hydrolysis rates under the experimental conditions.

The extent of reaction of the isotope effect reactions was followed by transferring an aliquot of the reaction solution into 0.1 N NaOH and assaying for *p*-nitrophenol by measuring the absorbance at 400 nm. Isotope effect experiments were carried out in triplicate. Reactions were stopped when the level of conversion of substrate was from 40 to 60%, and an aliquot was removed for determination of the precise fraction of reaction. This aliquot was split, with one portion analyzed immediately and the other portion placed in TRIS buffer at pH 9.0 with alkaline phosphatase for several hours. After this portion was analyzed, the ratio of *p*-nitrophenol in these two samples gave the extent of reaction.

Reactions were stopped by cooling on ice and titrating to pH 4, followed by extraction three times with an equivalent volume of diethyl ether to quantitatively remove the product *p*-nitrophenol. The aqueous layer containing the residual substrate was evaporated briefly under vacuum to remove dissolved ether, an equivalent volume of the TRIS pH 9.0 buffer added, and the pH adjusted to 9.0 with NaOH. This sample was treated with alkaline phosphatase to quantitatively hydrolyze all of the remaining substrate. This mixture was then titrated back to pH 5.0 and extracted with ether; the *p*-nitrophenol in this ether fraction represents the residual substrate from the enzymatic reaction. The ether fractions were dried over magnesium sulfate and filtered, and the solvent was removed by rotary evaporation. The *p*-nitrophenol was sublimed under vacuum at 90 °C, and 1.0−1.5 mg samples were prepared for isotopic analysis using an ANCA-NT combustion system in tandem with a Europa 20-20 isotope ratio mass spectrometer.

Isotope effects were calculated from the isotopic ratio in the *p*-nitrophenol product at partial reaction (R_p), in the residual substrate (R_s), and in the starting material (R_o). Equation 1 was used to calculate the observed isotope effect from R_p and R_o at fraction of reaction *f*. Equation 2 was used to calculate the observed isotope effect from R_s and R_o (*14*). Thus, each experiment yields two independent determinations of the isotope effect.

$$\text{isotope effect} = \log(1 - f)/\log[1 - f(R_p/R_o)] \quad (1)$$

$$\text{isotope effect} = \log(1 - f)/\log[(1 - f)(R_s/R_o)] \quad (2)$$

R_o was determined in two ways. Samples of unreacted substrate were subjected to analysis by isotope ratio mass spectroscopy, and as a control, these results were compared to those from *p*-nitrophenol isolated after complete hydrolysis of substrate using the isolation and purification procedures used in the isotope effect experiments. The agreement of these two numbers demonstrates that, within experimental error, no isotopic fractionation occurs as a result of the procedures used to isolate and purify the *p*-nitrophenol.

The ^{18}O isotope effects were measured by the remote-label method (*15*), as previously described for the solution reactions of *p*NPP (*12*). In these experiments, the nitrogen atom in the substrate is used as a reporter for isotopic changes at the bridging oxygen atom or the nonbridging oxygen atoms. These experiments yield an observed isotope effect which is the product of the effect due to ^{15}N and to ^{18}O substitutions. The observed isotope effects from these experiments were then corrected for the ^{15}N isotope effect and for incomplete levels of isotopic incorporation in the starting material, as previously described (*16*).

Steady State Kinetics Experiments with the Arg409 Mutant Yersinia PTPases. The *Yersinia* PTPase activity was assayed at 30 °C in a reaction mixture (0.2 mL) containing 10 mM *p*NPP as the substrate and 100 mM sodium acetate and 1 mM EDTA (pH 5.5); the ionic strength of the buffer was adjusted using NaCl to 0.15 M. The reaction was initiated by addition of enzyme and quenched after 2 min by addition of 1 mL of 1 N NaOH. The rate of nonenzymatic hydrolysis of the substrate was corrected by measuring the increase in optical density without the addition of enzyme. The amount of product (*p*-nitrophenol) was determined from the absorbance at 405 nm using a molar extinction coefficient of 18 000 M^{-1} cm^{-1} (*17*).

The effect of pH on the hydrolysis of *p*NPP catalyzed by the wild type as well as the Arg409 mutant *Yersinia* PTPases was investigated at 30 °C in pH-buffered solutions. Buffers that were used were as follows: pH 4.0−5.7, 100 mM acetate; pH 6.0−6.8, 50 mM succinate; pH 7.0−7.3, 50 mM 3,3-dimethylglutarate; and pH 7.5−8.0, 100 mM TRIS. All of the buffer systems contained 1 mM EDTA, and the ionic strength of the solution was kept at 0.15 M by adding NaCl. Initial rate measurements for the enzyme-catalyzed hydrolysis of *p*NPP were conducted as described above. Michaelis−Menten kinetic parameters were determined from a direct fit of the velocity versus [S] data to the Michaelis−Menten equation using the nonlinear regression program KinetAsyst (IntelliKinetics, State College, PA). pH dependence data were fitted to the appropriate equations using a nonlinear least-squares regression program.

RESULTS

Steady State Kinetics. Steady state kinetic parameters, k_{cat} and K_m, were measured for the wild type as well as for the R409A and R409K mutant *Yersinia* PTPases using *p*NPP as a substrate. Table 1 summarizes kinetic parameters of the wild type and the mutant enzymes at 30 °C and pH 5.0, 6.0, and 7.0. At the pH optimum (pH 5.0), mutation of Arg409 to Lys or to Ala results in decreases in k_{cat} of 46000- and

Table 1: Kinetic Parameters of the *Yersinia* PTPase and the Arg409 Mutants

pH	*Yersinia* PTPase	k_{cat} (s^{-1})	K_m (mM)	k_{cat}/K_m (s^{-1} mM^{-1})
	wild type	1200 ± 30	2.8 ± 0.20	430 ± 32
5.0	R409A	0.072 ± 0.005	67 ± 10	0.0011 ± 0.0002
	R409K	0.026 ± 0.004	5.1 ± 0.8	0.0051 ± 0.0011
	wild type	340 ± 12	2.4 ± 0.14	140 ± 9
6.0	R409A	0.040 ± 0.001	68 ± 11	0.00059 ± 0.00011
	R409K	0.017 ± 0.001	4.8 ± 0.09	0.0035 ± 0.0002
	wild type	35 ± 2	2.3 ± 0.11	15 ± 1.1
7.0	R409A	0.012 ± 0.001	56 ± 12	0.00021 ± 0.00005
	R409K	0.014 ± 0.001	4.4 ± 0.09	0.0032 ± 0.0002

17000-fold, respectively. At pH 6.0 and 30 °C, the k_{cat} values for R409K and R409A were 0.017 and 0.040 s^{-1}, respectively, which are 20000- and 8500-fold lower, respectively, than that of the wild type enzyme. The K_m values for R409K and R409A were 4.8 and 68 mM, respectively, which are 2- and 28-fold higher, respectively, than those of the wild type enzyme.

The pH dependencies of k_{cat} and k_{cat}/K_m for the hydrolysis of *p*NPP catalyzed by the *Yersinia* PTPase and the Arg409 mutant PTPases were compared. For the PTPase-catalyzed hydrolysis of aryl phosphates, the kinetic parameter k_{cat}/K_m monitors the first phosphoryl transfer step, i.e., the phosphoenzyme formation step (*9*−*11*). The k_{cat}/K_m−pH profile was bell-shaped for the wild type *Yersinia* PTPase-catalyzed *p*NPP reaction (*18*). The slope of the acidic limb was 2, which was attributed to the ionization of the active site nucleophile Cys403 and the second ionization of the substrate *p*NPP. The slope for the basic limb was −1, which was due to the ionization of the general acid Asp356 (pK_{EH} = 5.2). Because of the low activity of the Arg409 mutants and the reduced stability of the PTPase at pH <5, possible variations in the active site Cys403 ionization due to substitutions at Arg409 in the low-pH region of the k_{cat}/K_m−pH plot could not be observed. Nonetheless, kinetic parameters for R409A and R409K were obtained from pH 4.8 to 8.0, which allowed an assessment of the effect of Arg409 mutation on the functionality of the general acid Asp356. The k_{cat}/K_m−pH plot for the *p*NPP hydrolysis reaction catalyzed by R409A is shown in Figure 3. Like the wild type enzyme-catalyzed *p*NPP hydrolysis (*8*, *18*), k_{cat}/K_m for R409A decreased as the pH was raised above pH 5.0, most likely due to the deprotonation of the general acid Asp356, and reached a limiting non-zero plateau at pH >7.0. The pK_{EH} for the general acid Asp356 in the R409A mutant was determined to be 5.6 ± 0.1, which is 0.4 p*K* unit higher than that of the wild type enzyme (Figure 3). A similar ionization constant was determined from the k_{cat}−pH plot, suggesting that k_{cat} and k_{cat}/K_m for the R409A reaction followed the same phosphorylation step. Unlike the wild type and the R409A mutant PTPases, neither k_{cat} nor k_{cat}/K_m of the R409K-catalyzed *p*NPP reaction exhibited significant pH dependence from pH 4.8 to 8.0 (Table 1 and data not shown). Thus, the pH dependency of these mutants suggests that the Arg409 to Lys mutation likely abolishes the general acid catalysis, whereas the general acid may still be somewhat functional in the R409A mutant.

Steady state kinetic parameters for the W354A and W354F mutant *Yersinia* PTPases have previously been reported (*8*).

Kinetic Isotope Effects. The kinetic isotope effects were measured by the competitive method using an isotope ratio mass spectrometer. Since the competitive method gives isotope effects on *V*/*K* (*19*), the isotope effects reported are those for the first phosphoryl transfer step, from *p*NPP to the enzymatic Cys nucleophile, even though hydrolysis of the phosphoenzyme intermediate is the overall rate-limiting step.

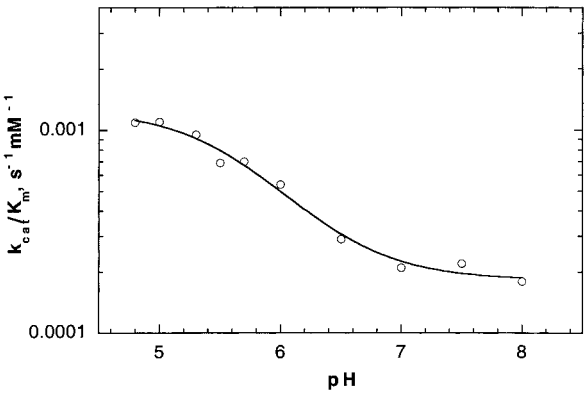

FIGURE 3: pH dependence of k_{cat}/K_m for the *p*NPP hydrolysis reaction catalyzed by the R409A mutant *Yersinia* PTPase. The rate profile indicates that both the EH and the E forms of the enzyme are catalytically active. To determine the pH-independent rate constants $(k_{cat}/K_m)_{EH}$ and $(k_{cat}/K_m)_E$, as well as the apparent ionization constants pK_{EH} (the pK_a of the general acid), the pH-dependent data were fitted to eq 3 $\{k_{cat}/K_m = [(k_{cat}/K_m)_{EH} + (k_{cat}/K_m)_E(K_{EH}/H)]/(1 + K_{EH}/H)\}$ using a nonlinear least-squares regression program (KaleidaGraph). pH-independent rate constants $(k_{cat}/K_m)_{EH}$ and $(k_{cat}/K_m)_E$ were 0.0013 ± 0.0001 and 0.00018 ± 0.00003 s^{-1} mM^{-1}, respectively. The group that must be protonated for catalysis has a pK_{EH} value of 5.6 ± 0.1.

Table 2: Isotope Effects of the Native Enzyme and Asp356, Trp354, and Arg409 Mutants

enzyme and pH	$^{15}(V/K)$	$^{18}(V/K)_{bridge}$	$^{18}(V/K)_{nonbridge}$
native enzyme	0.9999 (3)	1.0152 (6)	0.9998 (13)
D356N (pH 6)	1.0024 (5)	1.0275 (16)	1.0022 (5)
D356N (pH 9)	1.0026 (2)	1.0322 (6)	1.0021 (4)
W354A (pH 6)	1.0021 (2)	1.0310 (5)	1.0038 (5)
W354A (pH 9)	1.0021 (4)	1.0320 (6)	1.0036 (5)
W354F (pH 6)	1.0013 (2)	1.0240 (10)	1.0015 (8)
W354F (pH 9)	1.0022 (1)	1.0320 (10)	1.0039 (4)
R409K (pH 6)	1.0020 (5)	1.0273 (3)	1.0049 (7)
R409A (pH 6)	1.0012 (3)	1.0200 (5)	0.9990 (7)

Isotope effects were calculated as described in Materials and Methods and are reported in Table 2 with their standard errors in the last digit shown in parentheses. The ^{18}O isotope effects reported in this table have been corrected for the effect of the remote ^{15}N label and for levels of isotopic incorporation as previously described (*12*). Multiple determinations were made of each isotope effect, and the reported values are the averages from all experiments under the given sets of conditions. The isotope effects obtained from the isotopic ratios of product, and those obtained from the isotopic ratios of residual substrate, agreed within experimental error in all cases and were averaged together to give the results shown in Table 2.

The substrate for the enzymatic reaction is the dianion of *p*NPP; the pK_a of this compound has been reported as 5.0 ± 0.05 (*13*, *20*). Thus, in the isotope effect reactions conducted at pH 6.0, about 10% of the substrate was present in solution as the monoanion. Fractionation will occur between the monoanion and dianion species at the nonbridge oxygen position due to the isotope effect for deprotonation. This

isotope effect is 1.051 for a phosphate monoester (*21*). The observed values for $^{18}(V/K)_{nonbridge}$ in Table 2 have been corrected for this isotopic fractionation as previously described (*12*). Previously determined (*9*) isotope effects for the reactions of *p*NPP with native *Yersinia* PTPase and the D356N mutant are also reported in Table 2 to allow comparisons with the data from the study presented here.

DISCUSSION

Factors Influencing the Isotope Effects. The overall catalytic mechanism for PTPases is represented in Scheme 1. Because the competitive method was used to measure the isotope effects, they are effects on *V*/*K* and thus are effects on the part of the mechanism up to and including the first irreversible step, regardless of which step is rate-limiting in the overall enzymatic mechanism. Prior work with the PTPase from *Yersinia* has shown that the chemical step of phosphoryl transfer from *p*NPP to Cys403 is rate-limiting for *V*/*K*, both for the native enzyme and for general acid mutants (*9*). The kinetic isotope effects with the substrate *p*NPP are not suppressed by commitment factors, and are the intrinsic ones for the transition state of the phosphoryl transfer step (*9*).

Kinetic isotope effects can characterize reactions in detail, in particular yielding information about the structure of the transition state. In phosphoryl transfer reactions with *p*NPP, the isotope effects $^{15}(V/K)$ and $^{18}(V/K)_{bridge}$ measure the level of charge delocalization in the leaving group and the degree of P−O bond cleavage, respectively. The secondary $^{15}(V/K)$ effect arises from delocalization of charge into the aromatic ring, which involves contribution from a quinonoid resonance structure involving the nitro group (*22*). The primary isotope effect at the scissile P−O bond, $^{18}(V/K)_{bridge}$, gives a measure of the degree of cleavage of this bond in the transition state. Phosphate monoesters typically react via transition states characterized by extensive bond cleavage to the leaving group and only a small degree of bond formation to the nucleophile (*23*, *24*). The solution and enzymatic reactions of the dianion of *p*NPP exhibit bridge-^{18}O isotope effects in the range of 1.0202−1.030, and ^{15}N isotope effects of 1.0028−1.0039, when the leaving group departs as the negatively charged anion. Values at the upper end of these ranges represent isotope effects for nearly full P−O bond cleavage and a nearly full unit negative charge on the leaving group. When the leaving group is protonated in the transition state, as in the reactions of native PTPases, both of these isotope effects are reduced (*9*−*12*). Protonation of *p*-nitrophenol is associated with an inverse ^{18}O isotope effect of 0.985 (*25*). A transition state in which P−O bond cleavage and proton transfer are both far advanced would be expected to exhibit an observed $^{18}(V/K)_{bridge}$ isotope effect of about 1.015, which is the product of the 0.985 isotope effect for protonation and 1.03. This is very close to the value measured in reactions of *p*NPP with the native *Yersinia* enzyme (Table 2) (1.0152 ± 0.0006) (*9*) as well as with other native PTPases (*10*, *11*). If protonation is synchronous with P−O bond cleavage, the leaving group should remain neutral and the $^{15}(V/K)$ isotope effect should be near unity, which is the case in the reaction of the native enzyme (0.9999 ± 0.0003). As expected, the observed $^{18}(V/K)_{bridge}$ and $^{15}(V/K)$ isotope effects for the general acid deficient D356N mutant *Yersinia* PTPase-catalyzed reaction are similar to those for the solution reaction of the dianion of *p*NPP.

Calculations predict inverse values of $^{18}(V/K)_{nonbridge}$ for dissociative transition states and normal values for tighter transition states where the phosphoryl group resembles a phosphorane (*26*).[2] Reported nonbridge ^{18}O isotope effects for reactions of monoester dianions in solution (*12*) are small and inverse. Phosphate diesters and triesters have tighter transition states with considerable nucleophilic participation, and the nonbridge ^{18}O isotope effects for these compounds which have been reported are (with a single exception) normal, in the range of 1.0040−1.0250 (*27*, *28*). The small inverse value for $^{18}(V/K)_{nonbridge}$ measured for the reaction of the native *Yersinia* PTPase with *p*NPP (Table 2) is replaced by a small normal value in reactions of general acid mutants (Table 2). The same change is seen in the PTP1 (*9*) and Stp1 PTPase (*11*), as well as the dual-specificity phosphatase VHR (*10*), which all share essentially identical active sites. This change in the $^{18}(V/K)_{nonbridge}$ isotope effect suggests a transition state with more nucleophilic participation in the general acid mutants. Such a change is consistent with expectations from the Hammond postulate, where deactivation of the leaving group is predicted to result in a tighter transition state. The $^{18}(V/K)_{nonbridge}$ isotope effects for these reactions are smaller than those observed for diester and triester reactions in solution. The recent finding that mutations to the active site Arg409 leave the $^{18}(V/K)_{nonbridge}$ isotope effects essentially unaltered implies that isotope effects on binding are not significant, and that these isotope effects result from transition state effects (*29*). All three isotope effects for reactions of general acid mutants are similar to those on the solution hydrolysis of the monoester, and are very dissimilar to those of diester and triester reactions. This indicates that the enzymatic transition state is loose, similar to that of the dianion in solution, as has been discussed elsewhere (*9*, *30*).

In summary, all three isotope effects respond to protonation of the leaving group in the PTPase reaction. If movement of the WpD loop is hindered by a mutation in such a way that the extent of proton transfer in the transition state is reduced but not prevented, then the isotope effects should be intermediate between those observed when proton transfer is fully synchronized with P−O bond cleavage (as in the native enzyme) and those observed when the leaving group bears a full charge (as in the general acid mutant).

With this background, the isotope effects for the reactions of the *Yersinia* PTPase with mutations at W354 and R409 can be evaluated for the effect of these mutations on the function of the general acid in the transition state of the catalytic reaction.

[2] The secondary nonbridge ^{18}O isotope effects are not solely determined by bond order changes, but also by bending and torsional vibrational modes. The latter factors can be important in secondary isotope effects at atoms bonded to an atom that undergoes a hybridization change. Considerations of bond order changes alone would lead one to expect the $^{18}k_{nonbridge}$ isotope effect to be inverse for loose, dissociative transition states and normal for tight, associative ones. The bending modes might be in the opposite direction, however, by analogy with the normal α-secondary deuterium isotope effects that accompany carbon hybridization changes of the type sp^3 to sp^2 to sp^2 to sp. The trend in the data for numerous phosphate ester reactions suggests that bond order change is the dominant contributor to the $^{18}k_{nonbridge}$ isotope effect since these are normal for diester and triester reactions and inverse (though very small) for monoester reactions.

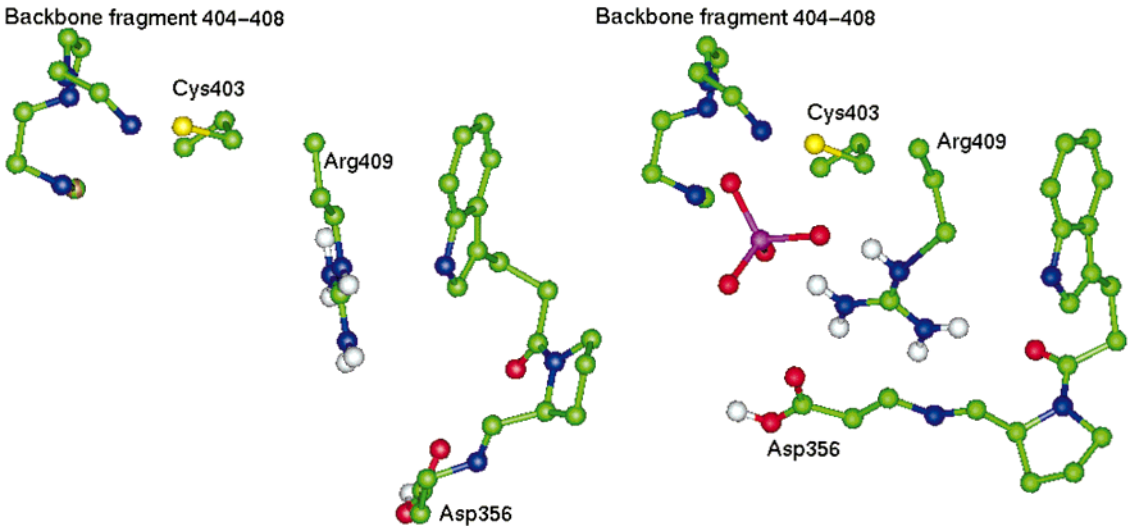

FIGURE 4: Orientations of groups at the active site of the *Yersinia* PTPase in the unbound state (left) and when sulfate is bound at the active site (right). Other oxyanions such as tungstate result in similar conformational changes. Hydrogen bonds are present between the oxyanion and backbone amide groups as well as with Arg409. This residue rotates to form two hydrogen bonds to the anionic group, resulting in the formation of a new hydrogen bond with the carbonyl oxygen atom of Trp354. The associated movement of the WpD loop brings Asp356 into position to function as a general acid during catalysis. The structures that are shown are from published X-ray structures (*6*, *31*) with computer-generated hydrogen atoms added to the Arg and Asp residues.

Effect of Mutation of Trp354 to Ala or Phe. In the reaction of W354A at pH 6.0, the isotope effects for the leaving group, $^{15}(V/K)$ and $^{18}(V/K)_{bridge}$, are very close to their values with the general acid mutant D356N. The same is true for $^{18}(V/K)_{nonbridge}$ where the change from the near unity value for this isotope effect seen in the native enzyme reaction to a small normal isotope effect mirrors the change induced by mutation of the general acid. These data indicate that protonation of the leaving group is eliminated by the W354A mutation and that the leaving group departs as the anion in the transition state of the catalytic reaction. In contrast, for the reaction of W354F at pH 6.0, each of the isotope effects is intermediate between those for D356N and those for the native enzyme where protonation of the leaving group in the transition state is intact. These data indicate that in the W354F mutant partial proton transfer in the transition state occurs but that protonation lags behind P−O bond cleavage, resulting in development of a partial negative charge on the leaving group.[3] At pH 9.0, the general acid will be almost entirely deprotonated and thus far less effective regardless of its ability to assume proper positioning. When the reactions of both W354A and W354F are examined at pH 9.0, the isotope effects for W354A are unchanged while those for W354F increase and are now equal to those for W354A and to those of D356N. This confirms that the general acid, while impaired, is still partially functioning in the transition state of the reaction with the W354F mutant at pH 6.0.

Corroborating evidence for the difference in the extent of acid catalysis in these two mutants is seen in their reported variations of k_{cat} with pH (*8*). The W354A mutant exhibits a pH−rate profile similar in shape to that of D356N (*5*), in which the bell-shaped profile of the native enzyme is replaced with a half-bell comprised of an acidic limb and a plateau above pH 5.0. In addition, the k_{cat} and k_{cat}/K_m kinetic parameters of the W354A reaction with *p*NPP are similar to those with D356N. By contrast, the W354F pH−rate profile (*8*) exhibits an acidic limb and a maximum at pH 5.0, and then a small decrease between pH 5.0 and 6.5 followed by the same plateau value seen with W354A. The decrease in rate between pH 5.0 and 6.5 indicates that some contribution from general acid catalysis exists in this mutant.

The differential effects of the two mutations can be rationalized by an examination of the structure of the enzyme. X-ray structures (*7*) show that when an oxyanion such as sulfate binds at the active site, the Arg409 residue moves to form bidentate hydrogen bonds with two oxygen atoms of the anion (Figure 4). Conformational changes in the active site result in the formation of a new hydrogen bond between the guanidinium group of Arg409 and the carbonyl oxygen atom of Trp354. As a result, the indole ring of Trp354 moves into a hydrophobic crevice, making van der Waals contacts with the aliphatic portion of Arg409 (Figure 5) (*7*). These interactions are associated with movement of the WpD loop in attaining the closed position when the oxyanion is bound. The mutation to Phe leaves a side chain that is reasonably isosteric with the indole moiety in the native enzyme, which evidently is sufficient to facilitate movement of the loop to bring the general acid into position for partial proton transfer in the transition state. Mutation to Ala completely removes these van der Waals contacts. Both the pH−rate data and

[3] An astute reviewer raised the possibility of an alternative model in which there are two populations of enzyme, one in which full protonation is present and one in which protonation is absent. This model would result in a similar pattern in the observed isotope effects if the two forms of the enzyme have similar activities at pH 6. The two models predict different behavior of the rate constant as a function of the pK_a of the leaving group. If there is a single active form of the enzyme in which partial protonation occurs, a linear Brønsted $\beta_{leaving\ group}$ slope intermediate between that of the native enzyme and the general acid mutant should be observed. If two active forms of the enzyme are performing catalysis, a similar slope is predicted, but as the leaving group pK_a increases, the enzyme form lacking general acid catalysis should contribute progressively less to catalysis, resulting in curvature of the Brønsted plot. The $\beta_{leaving\ group}$ plots for W354F (at pH 5.5) and R409A (at pH 6.0) are linear and are indeed midway between the slopes of the native enzyme and the general acid mutant D356N (data not shown). The $\beta_{leaving\ group}$ values for W354A and R409K are similar to that of D356N. We interpret the lack of curvature as favoring the model in which a single active form of the enzyme is operative.

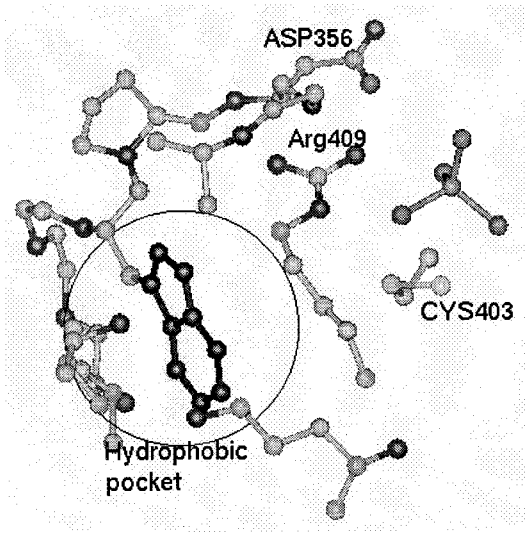

FIGURE 5: Hydrophobic pocket occupied by the indole moiety of Trp354 in the native enzyme when an oxyanion such as sulfate is bound (*31*).

isotope effect data indicate that functioning of the general acid, and, by inference, movement of the WpD loop, is partially effective in the W354F mutant and completely ineffective in the W354A mutant.

Effect of Mutation of Arg409 to Ala or Lys. The Arg409 residue assists not only in substrate binding and transition state stabilization but also in the conformational changes described previously which accompany binding and play a role in the movement of the WpD loop. Binding of substrate also is assisted by formation of hydrogen bonds to backbone amide groups in the active site (Figure 6a). Comparison of the crystal structure of the free enzyme and structures with oxyanions bound shows that these backbone amide groups also undergo movement upon binding of oxyanions.

In the R409K mutant, an ammonium group replaces the guanidinium group. Both the position of the cationic atom and that of the Lys residue's hydrogen bonds in the active site are necessarily different from their positions in the guanidinium group of Arg409 in the native enzyme (Figure 6b). In the R409A mutant, the Arg side chain is reduced to a methyl group (Figure 6c). The K_m values for R409K and R409A were 4.8 and 68 mM, respectively, at pH 6.0, compared with the value of 2.4 mM for the native enzyme. The R409K and R409A mutants exhibit k_{cat} values of 0.040 and 0.017 s^{-1}, respectively. These values are about 10^4-fold lower than that for the native enzyme, but are still nearly 10^5-fold faster than the uncatalyzed rate of hydrolysis of *p*NPP.

Although both Lys and Ala substitutions for Arg409 resulted in a huge decrease in catalytic activity, the R409K- and R409A-catalyzed reactions exhibited different pH dependencies. The R409K-catalyzed initial phosphoryl transfer (as defined by k_{cat}/K_m) was more efficient than that of the R409A reaction, yet the former reaction exhibited no pH dependence. The absence of a pH dependence on the rate suggests that Asp356 is not functional as a general acid in R409K. All three isotope effects for the reaction of the R409K mutant are similar to their values in D356N, which also indicates that this mutation results in the disabling of general acid catalysis. However, the k_{cat}/K_m for R409K (0.0035 s^{-1} mM^{-1}) is still 80-fold lower than that of D356N (0.28 s^{-1} mM^{-1}), from which the general acid has been removed. The observed reduction in the catalytic efficiency of R409K is thus likely the combined effect of the elimination of the general acid and the possible decreased level of transition state interactions with the phosphoryl oxygens due to the Arg to Lys mutation.

In contrast, general acid catalysis by Asp356 appears to be operable in R409A as judged by the pH−rate profile (Figure 3) and the isotope effect data. The latter data indicate that although proton transfer occurs in the transition state, it is not as advanced as in the native enzyme and lags behind P−O bond cleavage. The result is a partial net negative charge that is borne by the leaving group (see footnote 3). Thus, the decrease in catalytic activity for the R409A mutant may be primarily the result of the loss of transition state stabilization from the guanidinium side chain, with some contribution arising from less efficient protonation of the leaving group.

It is interesting, and somewhat counterintuitive, that mutation of Arg to Ala should be less disabling to movement of the WpD loop than mutation of this residue to Lys. A possible explanation is that while in the Lys mutant a positively charged residue capable of donating hydrogen bonds remains present, the interactions are positioned differently than those in the native enzyme. Thus, in R409K, the Lys residue interacts with the substrate and/or Trp354 in a "nonproductive" fashion that may disrupt the proper positioning of the substrate and the associated induced WpD loop closure. In contrast, in the Ala mutant, a small residue resides in this position that is completely incapable of direct interactions with the phosphoryl group and the Trp354 residue. Hydrogen bonding interactions with the backbone amide residues will remain, although the positioning of the WpD loop and the general acid Asp356 may not be as optimal as in the native enzyme. The data for the two Arg409 mutants suggest that eliminating the interactions with the Arg residue is less deleterious to the conformational changes accompanying general acid catalysis than substitution with a residue that forms hydrogen bonding and electrostatic interactions in a different, improper geometry.

Effect of pH on the Isotope Effects of the Native Enzyme Reaction. The isotope effects for the reaction of the native enzyme with *p*NPP were evaluated at pH ≥5.5 (Table 3). In particular, we were interested in the $^{15}(V/K)$ isotope effect, which would be expected to increase as the pH was raised to values at which the general acid would be deprotonated and thus unable to transfer a proton to the leaving group. The results show that indeed the value of $^{15}(V/K)$ did increase as the pH was raised from pH 5.5 to 10.5 but not as rapidly nor to as large a final magnitude as might be expected. The values never become as large as that for the D356N mutant (1.0024 at pH 6.0). One explanation for the slow rise in the magnitude of this isotope effect lies in the relative values for k_{cat} for the native enzyme and for the reaction with the general acid disabled. The D356N mutant has a value for k_{cat} which is 1700-fold smaller than that for the native enzyme. The value for k_{cat} of D356N should be a reasonable estimate for the rate constant for the reaction of the native enzyme form in which the general acid is rendered nonfunctional by deprotonation. The Asp has been found to have a pK_a of about 5.2 in the native enzyme. Thus, at pH 8.5 only about $^1/_{1700}$ of the enzyme will be in the correct

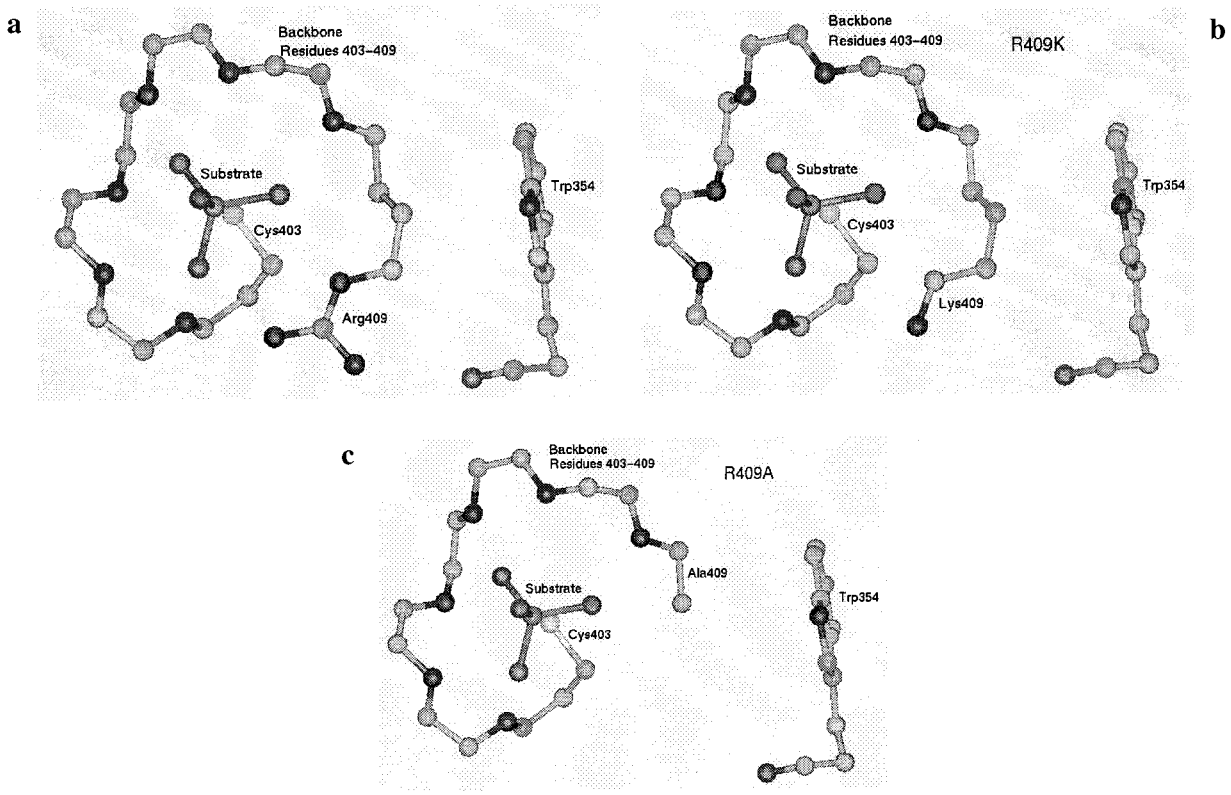

FIGURE 6: View of the active site with bound sulfate, showing hydrogen bonding contacts with backbone amide groups (*31*). The nucleophilic Cys403 is behind the sulfate; from this view in the catalytic reaction, the leaving group would be pointed toward the viewer. In panel a, hydrogen bond contacts are also made with Arg409. In panel b, the ammonium group of lysine replaces the guanidinium group; the ammonium group retains the potential to affect the binding and positioning of the substrate. Panel c shows the corresponding R409A mutant that retains only interactions with backbone amide residues for these roles. The structures shown in panels b and c were derived by simple molecular replacement and have not been minimized.

Table 3: Variation of Isotope Effects of Native Enzyme with pH

pH	$^{15}(V/K)$	$^{18}(V/K)_{bridge}$	$^{18}(V/K)_{nonbridge}$
5.0	0.9999 (3)	1.0152 (6)	0.9998 (13)
6.0	0.9999 (3)	1.0160 (15)	1.0001 (13)
8.5	1.0008 (3)		
8.75	1.0011 (2)		
9.0	1.0010 (1)	1.0214 (5)	1.0021 (3)
9.5	1.0016 (2)		
10.0	1.0019 (1)		

protonation state for general acid catalysis to occur. However, pH−rate data (*18*) show that the rate constant for the correctly protonated form of the enzyme will also be 1700 times larger than that for the deprotonated form. Thus, at this pH, one expects that about half of the turnover will be from the correctly protonated form of the enzyme and the value for $^{15}(V/K)$ should be about midway between that observed when the general acid is fully functioning and that when it is deleted by mutation. The value of $^{15}(V/K)$ at pH 8.5 is about $^1/_3$ of the maximal value seen when no general acid catalysis occurs. Given the small magnitudes of this isotope effect, this is in reasonable agreement with the prediction.

At still higher pH values, it is expected that this isotope effect should rapidly approach that for D356N. However, the $^{15}(V/K)$ isotope effect increases only slowly above this pH and never reaches that seen in the reaction with D356N. We are not certain of the reasons for this behavior. It was noted that at pH values above 9.0 the enzyme is much less stable in solution and gradual precipitation is increasingly evident. This indicates that pH levels above 9.0 result in conformational perturbations to the enzyme, and thus, data from reactions above this pH must be interpreted with caution. Due to the large amounts of enzyme needed for the experiments, only the $^{15}(V/K)$ effect was measured across this full pH range; $^{18}(V/K)_{bridge}$ and $^{18}(V/K)_{nonbridge}$ were measured only at pH 6.0 and 9.0. These two isotope effects exhibited a similar trend toward the values seen with the D356N mutant. At pH 9.0, $^{18}(V/K)_{bridge}$ is about halfway between that of the native enzyme at the pH optimum and that of D356N. The value for $^{18}(V/K)_{nonbridge}$ at this pH is identical within experimental error to that of D356N.

The isotope effects for D356N were also measured at pH 9.0. The magnitudes of $^{15}(V/K)$ and $^{18}(V/K)_{nonbridge}$ were unchanged from those observed at pH 6.0. The value for $^{18}(V/K)_{bridge}$ is increased somewhat at pH 9.0. The reason for the small increase is uncertain.

CONCLUSIONS

Mutations to hinge residue Trp354 affect the functioning of the general acid residue in catalysis by the *Yersinia* PTPase. Mutation of Trp354 to Ala completely disables general acid catalysis, and the leaving group departs with essentially a full negative charge. In the Phe mutant, partial acid catalysis occurs with the proton only approximately half transferred in the transition state with a resulting partial negative charge on the leaving group in the transition state. In contrast in the native enzymatic reaction, protonation is completely synchronous with P−O bond cleavage and the leaving group remains uncharged. The results are indicative

of impaired positioning of the flexible WpD loop in both of these mutants, and are consistent with the observation that while W354A has a k_{cat} value that is reduced 480-fold from that of the native enzyme, W354F is slowed only 200-fold.

Mutation of Arg409 to either Lys or Ala results in a substantially reduced rate of catalytic turnover. The K_m of the R409K mutant with *p*NPP is doubled from that of the wild type enzyme, while that for R409A is increased 30-fold. However, functioning of general acid catalysis in the R409K mutant is completely abolished, while partial proton transfer in the transition state still occurs in the R409A mutant. The lowered catalytic efficiency resulting from the R409K mutation is due to a combination of a reduction in the extent of transition state interactions with the phosphoryl oxygens and from disruption to the functioning of the general acid catalyst. The reduction in catalytic efficiency in the R409A mutant is likely due primarily to the loss of transition state stabilization arising from the loss of the guanidinium group.

REFERENCES

1. Zhang, Z.-Y. (1998) *CRC Crit. Rev. Biochem. Mol. Biol. 33*, 1−52.
2. Zhang, Z.-Y., Wang, Y., Wu, L., Fauman, E., Stuckey, J. A., Schubert, H. L., Saper, M. A., and Dixon, J. E. (1994) *Biochemistry 33*, 15266−15270.
3. Cho, H., Krishnaraj, R., Kitas, E., Bannwarth, W., Walsh, C. T., and Anderson, K. S. (1992) *J. Am. Chem. Soc. 114*, 7296−7298.
4. Guan, K. L., and Dixon, J. E. (1990) *Science 249*, 553−556.
5. Zhang, Z.-Y., Wang, Y., and Dixon, J. E. (1994) *Proc. Natl. Acad. Sci. U.S.A. 91*, 1624−1627.
6. Stuckey, J. A., Schubert, H. L., Fauman, E. B., Zhang, Z.-Y., Dixon, J. E., and Saper, M. A. (1994) *Nature 370*, 571−575.
7. Schubert, H. L., Fauman, E. B., Stuckey, J. A., Dixon, J. E., and Saper, M. A. (1995) *Protein Sci. 4*, 1904−1913.
8. Keng, Y.-F., Wu, L., and Zhang, Z.-Y. (1999) *Eur. J. Biochem. 259*, 809−814.
9. Hengge, A. C., Sowa, G. A., Wu, L., and Zhang, Z.-Y. (1995) *Biochemistry 34*, 13982−13987.
10. Hengge, A. C., Denu, J. M., and Dixon, J. E. (1996) *Biochemistry 35*, 7084−7092.
11. Hengge, A. C., Zhao, Y., Wu, L., and Zhang, Z.-Y. (1997) *Biochemistry 36*, 7928−7936.
12. Hengge, A. C., Edens, W. A., and Elsing, H. (1994) *J. Am. Chem. Soc. 116*, 5045−5049.
13. Bourne, N., and Williams, A. (1984) *J. Org. Chem. 49*, 1200−1204.
14. Bigeleisen, J., and Wolfsberg, M. (1958) *Adv. Chem. Phys. 1*, 15−76.
15. O'Leary, M. H., and Marlier, J. F. (1979) *J. Am. Chem. Soc. 101*, 3300−3306.
16. Caldwell, S. R., Raushel, F. M., Weiss, P. M., and Cleland, W. W. (1991) *Biochemistry 30*, 7444−7450.
17. Wu, L., and Zhang, Z.-Y. (1996) *Biochemistry 35*, 5426−5434.
18. Zhang, Z.-Y., Malochowski, W. P., Van Etten, R. L., and Dixon, J. E. (1994) *J. Biol. Chem. 269*, 8140−8145.
19. Northrop, D. B. (1977) in *Isotope Effects on Enzyme-Catalyzed Reactions* (Cleland, W. W., O'Leary, M. H., and Northrop, D. B., Eds.) p 122, University Park Press, Baltimore, MD.
20. Massoud, S. S., and Sigel, H. (1988) *Inorg. Chem. 27*, 1447−1453.
21. Knight, W. B., Weiss, P. M., and Cleland, W. W. (1986) *J. Am. Chem. Soc. 108*, 2759−2761.
22. Hengge, A. C., and Cleland, W. W. (1990) *J. Am. Chem. Soc. 112*, 7421−7422.
23. Thatcher, G. R. J., and Kluger, R. (1989) *Adv. Phys. Org. Chem. 25*, 99−265.
24. Hengge, A. C. (1998) in *Comprehensive Biological Catalysis: A Mechanistic Reference* (Sinnott, M., Ed.) pp 517−542, Academic Press, San Diego, CA.
25. Hengge, A. C., and Hess, R. A. (1994) *J. Am. Chem. Soc. 116*, 11256−11263.
26. Weiss, P. M., Knight, W. B., and Cleland, W. W. (1986) *J. Am. Chem. Soc. 108*, 2761−2762.
27. Hengge, A. C., and Cleland, W. W. (1991) *J. Am. Chem. Soc. 113*, 5835−5841.
28. Hengge, A. C., Tobin, A. E., and Cleland, W. W. (1995) *J. Am. Chem. Soc. 117*, 5919−5926.
29. Hoff, R. H., Wu, L., Zhou, B., Zhang, Z.-Y., and Hengge, A. C. (1999) *J. Am. Chem. Soc. 121*, 9514−9521.
30. Alhambra, C., Wu, L., Zhang, Z.-Y., and Gao, J. (1998) *J. Am. Chem. Soc. 120*, 3858−3866.
31. Fauman, E. B., Yuvaniyama, C., Schubert, H., Stuckey, J. A., and Saper, M. A. (1996) *J. Biol. Chem. 217*, 18780−18788.

BI991570I